Progressive aggregation despite chaperone associations of a mutant SOD1-YFP in transgenic mice that develop ALS

Jiou Wang[a,b,1], George W. Farr[a,b,1], Caroline J. Zeiss[c], Diego J. Rodriguez-Gil[d], Jean H. Wilson[c], Krystyna Furtak[a,b], D. Thomas Rutkowski[e,2], Randal J. Kaufman[e], Cristian I. Ruse[f], John R. Yates III[f], Steve Perrin[g], Mel B. Feany[h], and Arthur L. Horwich[a,b,3]

[a]Howard Hughes Medical Institute, [b]Department of Genetics, [c]Section of Comparative Medicine, and [d]Department of Neurosurgery, Yale University School of Medicine, New Haven, CT 06510; [e]Howard Hughes Medical Institute and Department of Biological Chemistry, University of Michigan Medical Center, Ann Arbor, MI 48109; [f]Department of Chemical Physiology, The Scripps Research Institute, La Jolla, CA 92037; [g]ALS Therapeutic Development Institute, Cambridge, MA 02142; and [h]Department of Pathology, Brigham and Women's Hospital, Harvard Medical School, Boston, MA 02115

Contributed by Arthur L. Horwich, December 20, 2008 (sent for review November 3, 2008)

Recent studies suggest that superoxide dismutase 1 (SOD1)-linked amyotrophic lateral sclerosis results from destabilization and misfolding of mutant forms of this abundant cytosolic enzyme. Here, we have tracked the expression and fate of a misfolding-prone human SOD1, G85R, fused to YFP, in a line of transgenic G85R SOD1-YFP mice. These mice, but not wild-type human SOD1-YFP transgenics, developed lethal paralyzing motor symptoms at 9 months. In situ RNA hybridization of spinal cords revealed predominant expression in motor neurons in spinal cord gray matter in all transgenic animals. Concordantly, G85R SOD-YFP was diffusely fluorescent in motor neurons of animals at 1 and 6 months of age, but at the time of symptoms, punctate aggregates were observed in cell bodies and processes. Biochemical analyses of spinal cord soluble extracts indicated that G85R SOD-YFP behaved as a misfolded monomer at all ages. It became progressively insoluble at 6 and 9 months of age, associated with presence of soluble oligomers observable by gel filtration. Immunoaffinity capture and mass spectrometry revealed association of G85R SOD-YFP, but not WT SOD-YFP, with the cytosolic chaperone Hsc70 at all ages. In addition, 3 Hsp110's, nucleotide exchange factors for Hsp70s, were captured at 6 and 9 months. Despite such chaperone interactions, G85R SOD-YFP formed insoluble inclusions at late times, containing predominantly intermediate filament proteins. We conclude that motor neurons, initially ''compensated'' to maintain the misfolded protein in a soluble state, become progressively unable to do so.

Hsc70 | Hsp110 | motor neuron | neurodegeneration | proteomic

Amyotrophic lateral sclerosis (ALS) is a paralyzing neurodegenerative condition associated with production of ubiquitin-positive aggregates in motor neurons in both sporadic and inherited cases (1, 2). The nature of pathogenesis remains poorly understood, but in at least one inherited form of the condition, involving mutations in the abundantly expressed cytosolic homodimeric enzyme superoxide dismutase (SOD1), there is increasing evidence that protein misfolding is involved. In particular, disease-associated mutations affecting a variety of residues in different regions of the SOD1 subunit all lead to destabilization and misfolding (3–6), and in both humans and transgenic mice carrying such alleles, the enzyme subunit itself is found lodged in spinal cord aggregates (1, 2). This gain of function behavior is consistent with the generally dominant inheritance pattern of SOD1-linked ALS. By contrast, a loss of function behavior that might be attributed to deficiency of free radical scavenging function of the enzyme has not been supported: For example, many ALS-linked SOD1 alleles retain enzymatic activity (1, 2) and SOD1 knockout mice fail to develop motor disease (7).

The fate of mutant SOD1 protein is thus of major interest with respect to disease pathogenesis, and tracking the protein in vivo would seem desirable. Such an approach has recently been taken in cultured cells, where ALS-associated mutant versions of human SOD1 were fused with yellow fluorescent protein (YFP), enabling optical tracking of SOD1 aggregation (8). Aggregation of these fusion proteins was evidently a consequence of misfolding of the mutant SOD1 moiety, because a wild-type SOD1-YFP fusion did not form aggregates. We wished to address whether a similar mutant SOD1-YFP fusion protein expressed in mice would produce an ALS phenotype. If so, this could enable several avenues of investigation: fluorescent reporting in vivo of the distribution of expression and aggregation of the misfolded protein; fluorescent monitoring to facilitate purification of SOD1-YFP aggregates from spinal cord, allowing identification of the protein constituents; and immunoaffinity capture of soluble fusion protein species, including soluble oligomers, through the fluorescent protein moiety, allowing identification of associating proteins. We report here on such studies.

Results

Transgenic Mice Expressing a G85R SOD1-YFP Fusion But Not WT SOD1-YFP Develop ALS-Like Disease. We produced strains of transgenic mice expressing fusion proteins, either G85R SOD1-YFP (G85R SOD-YFP) or wild-type SOD1-YFP (WT SOD-YFP), formed by fusing the respective cloned human SOD1 gene through its C-terminal coding sequence in exon 5 to the YFP coding sequence (Fig. S1). G85R SOD1 is a misfolded mutant of SOD1 that has been associated with ALS disease in humans and transgenic mice (9, 10). Because SOD1 (hereafter referred to as SOD) is broadly expressed, we were readily able to identify transgenic SOD-YFP animals and genotype them based on the fluorescence of the pups' skin before growth of fur. Animals heterozygous for G85R SOD-YFP transgene insertions did not develop symptoms, but when homozygous, 2 lines with strong

Author contributions: J.W., G.W.F., C.J.Z., D.R.G., D.T.R., R.J.K., C.I.R., J.R.Y., M.B.F., and A.L.H. designed research; J.W., G.W.F., C.J.Z., D.R.G., J.H.W., K.F., D.T.R., C.I.R., M.B.F., and A.L.H. performed research; C.I.R., J.R.Y., and S.P. contributed new reagents/analytic tools; J.W., G.W.F., C.J.Z., D.R.G., D.T.R., R.J.K., C.I.R., M.B.F., and A.L.H. analyzed data; and J.W., G.W.F., and A.L.H. wrote the paper.

The authors declare no conflict of interest.

Freely available online through the PNAS open access option.

[1]J.W. and G.W.F. contributed equally to this work

[2]Present address: Department of Anatomy and Cell Biology, University of Iowa Carver College of Medicine, Iowa City, IA 52242

[3]To whom correspondence should be addressed. E-mail: arthur.horwich@yale.edu.

This article contains supporting information online at www.pnas.org/cgi/content/full/0813045106/DCSupplemental.

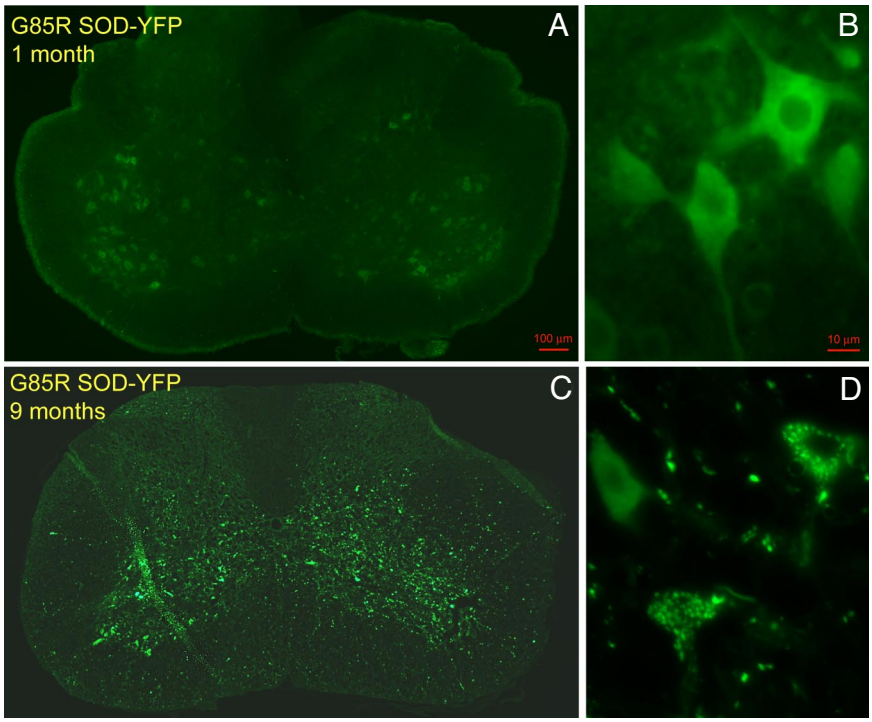

Fig. 1. Fluorescent images of spinal cord cross-sections from a 1-month-old G85R SOD-YFP mouse and from a 9-month-old G85R SOD-YFP animal with motor symptoms. Cords were rapidly dissected, embedded in OCT, frozen, sectioned in a cryotome, and transferred to a glass slide. The slides were then examined by fluorescence microscopy. Shown are low (*A* and *C*) and higher (*B* and *D*) magnification views of the same sections, showing diffuse fluorescence in large neuron cell bodies in the young animal, and punctate fluorescence both within cell bodies and outside of them in the symptomatic animal.

fluorescence, referred to as 641 and 737, developed motor neuron disease before a year of age. The age of onset of visible motor dysfunction in homozygous 641 animals was consistently 9 months, whereas onset in homozygous 737 animals varied from 4 months to 12 months. This correlated in Southern blot analyses with 641 carrying a single (multicopy) transgene insertion, whereas 737 proved to carry multiple insertions, such that motor symptoms occurred at the earliest ages when the greatest number of insertions were present (data not shown). WT SOD-YFP transgenics, in contrast, did not exhibit disease out to beyond 2 years, even when homozygous for transgene insertions that produced a higher steady-state level of fusion protein in spinal cord than achieved with G85R SOD-YFP. Because of the reproducible trajectory of disease, homozygous 641 animals were studied in detail.

Fluorescent Aggregates in Motor Neuron Cell Bodies and Processes in Spinal Cords of Symptomatic Animals. When the spinal cord from a 1-month-old 641 G85R SOD-YFP animal was rapidly fixed and examined in cross-section, strong but diffuse fluorescence was observed in large cell bodies in the gray matter (Fig. 1*A*), most abundantly in the anterior horn, with such fluorescence observed at higher magnification to extend into processes (Fig. 1*B*). The same pattern was also observed at 6 months of age (Fig. S2*a*). When spinal cord from a symptomatic animal of 9 months age was examined, an entirely different pattern was observed, with intense punctate fluorescent staining now observed in the gray matter (Fig. 1*C*), and with many neuron cell bodies containing punctate green fluorescent aggregates (Fig. 1*D*). Additional punctate aggregates localized in the neuropil (Fig. 1*D*), in some cases in contiguous processes. In comparison with the spinal cords from G85R SOD-YFP animals, cords from WT SOD-YFP animals from multiple lines of different ages up to 1 year, some exhibiting greater levels of total steady-state SOD-YFP protein in Western blot analysis, exhibited only low levels of fluorescence (Fig. S2*b*) and, at higher magnification, exhibited only a small amount of fluorescence in large neuron cell bodies (e.g., Fig. S2*c*).

Ubiquitin and GFAP Reactivity. When spinal cords were fixed and stained with anti-SOD antiserum, the same patterns as had been observed with fluorescence were obtained (Fig. S3*a*). Cords were also stained with anti-ubiquitin antibodies (Fig. S3*b*), revealing no significant staining in cords of 6-month-old G85R SOD-YFP animals or WT SOD-YFP animals but a distribution pattern in symptomatic 9-month-old mutant cord corresponding to that of the fluorescent aggregates, with punctate staining both within motor neuron cell bodies and outside. Ubiquitin-positive staining is classically observed in symptomatic conditions of both sporadic and SOD-linked ALS (1, 2). In parallel with late development of ubiquitin-positive staining, the gray matter of symptomatic 9-month-old G85R SOD-YFP animals, but not of 6-month-old animals, stained positively for GFAP, reflecting a glial response (Fig. S3*c*). In EM studies of a symptomatic G85R SOD-YFP animal, aggregates were observed in many motor neuron cell bodies (23/50) but not in astrocyte cell bodies (0/50) (representative image of mutant in Fig. S4). In additional fluorescence analysis of symptomatic animals, fluorescent aggregates were observed in ventral nerve root axons (Fig. S5), with a higher density observed proximally relative to distally, for example, in sciatic nerve.

In Situ RNA Hybridization Reveals That SOD Transgenes Are Expressed Predominantly in Motor Neurons in the Spinal Cord. The selective fluorescence of large motor neuron cell bodies in the spinal cord of G85R SOD-YFP transgenic animals raised a consideration of whether neurons are the principal site of expression of the fusion protein. To address this question, we carried out in situ RNA

hybridization, using a YFP probe, which distinguishes transcription of the transgene from that of endogenous SOD1. This revealed prominent expression in large cell bodies in the gray matter of both presymptomatic (data not shown) and symptomatic G85R SOD-YFP animals but also in WT SOD-YFP transgenic animals (Fig. S6). Minimal staining was observed in smaller cell bodies. The strong expression of the RNA in neurons, including motor neurons, is consistent with neurons as the major site of SOD-YFP protein in the transgenic animals (Fig. 1). This would imply that the fluorescent aggregates in the neuropil of symptomatic animals are likely to lie within neuronal processes.

Biochemical Fractionation Reveals Progressive Formation of Soluble Oligomers and Aggregates. ***Solubility.*** The fate of the G85R SOD-YFP protein over the course of disease progression was tracked by steps of fractionation. First, homogenization of spinal cord from either G85R SOD-YFP or WT SOD-YFP transgenic animals was carried out under native conditions, followed by centrifugation ($17{,}000 \times g \times 15$min). In Western blot analysis, using a polyclonal anti-YFP antibody, we observed that all of the fusion protein (43 kDa) was present in the soluble fraction of both WT SOD-YFP animals and 1-month-old G85R SOD-YFP animals (Fig. 2*A Left*). Similarly, when cords from wild-type animals of any age were analyzed, the protein was entirely soluble (data not shown). However, in spinal cord from 6-month-old G85R SOD-YFP animals, ≈25% of the protein was recovered in the insoluble fraction, and from 9-month-old symptomatic animals, ≈50% of the fusion protein was localized in the insoluble fraction. Thus, the mutant fusion protein becomes progressively less soluble with age.

G85R-YFP behaves as a misfolded monomer. To further evaluate the behavior of the G85R SOD-YFP protein, the soluble fractions from spinal cords of animals of the various ages were subjected to gel filtration chromatography on Superose 6, monitored with in-line fluorescence (Fig. 2*B*). First we evaluated a symptomatic G85R SOD-YFP animal, comparing it with a WT SOD-YFP one. Whereas SOD-YFP from wild-type cord eluted at the position of a dimer (≈80–90 kDa), corresponding to the homodimeric state that is observed for nonfused native wild-type SOD, mutant G85R SOD-YFP exhibited a major fluorescent peak at a position corresponding to SOD-YFP monomer (≈45 kDa), suggesting that dimerization of the mutant fusion protein had failed to occur. This failure of assembly is consistent with observations of Marklund and coworkers examining spinal cord of transgenic mice with nonfused G85R SOD (11).

To address whether the unassembled G85R SOD-YFP was properly folded, we assessed whether the disulfide bond normally present in native SOD (Cys-57–146) had been formed in the fusion protein from mutant animals. Tissue extracts were prepared in the presence of iodoacetamide to block free thiols, then the migration of the fusion protein was analyzed in SDS/PAGE in the absence or presence of DTT (Fig. 2*C*). As observed in earlier studies, if the disulfide is present, then the protein migrates more rapidly under nonreducing conditions (−DTT) than under reducing conditions (+DTT), whereas if the disulfide has not been formed, then the protein migrates at the "reduced" position in both the absence and presence of DTT. Whereas SOD-YFP from cord of wild-type animals exhibited differential migration reflecting the presence of the disulfide bond (Fig. 2*C Left*), the fusion protein from mutant animals, including animals at 1 month of age, exhibited relatively slower migration, corresponding to the reduced protein, both in the absence and presence of DTT (Fig. 2*C Right*). The lack of disulfide bond formation in G85R SOD-YFP corresponds once again to behavior observed for nonfused G85R SOD from spinal cord of transgenic mice (12). We conclude that G85R in either the nonfused or YFP-fused context is a misfolded monomeric protein.

Soluble oligomers of G85R SOD-YFP at 6 and 9 months. We noticed that a "shoulder" of fluorescence between 25 and 30 min of elution, corresponding to higher molecular weight species, was present in the gel filtration analysis of the symptomatic mutant animal (Fig. 2*B*, red trace), and analyzed these fractions by immunoblotting with anti-YFP antibodies (Fig. 2*D*). In WT SOD-YFP animals and in 1-month-old mutant animals, the fusion protein migrated at lower molecular masses, corresponding to the sizes of the dimer or monomer forms, respectively. Strikingly, however, when mutant animals of 6 months or 9 months of age were examined, the fusion was detected in higher molecular weight fractions, with a portion of the material from the 9-month-old found at the void volume of the column, corresponding to 4–6 MDa. Thus, there is an age-dependent progression in the formation of soluble oligomers in parallel with progressive production of insoluble protein. These two states likely comprise a precursor-product relationship. These data raised questions both about whether there are cellular components associating with soluble misfolded G85R SOD-YFP and about the composition of the end-state insoluble aggregates. These were addressed using proteomic analyses.

Physical Associations of Soluble G85R SOD-YFP in Spinal Cord—Strong Association with Hsc70 at All Ages and Association with 3 Hsp110 Proteins at Later Times. To detect physical association of soluble G85R SOD-YFP with other proteins, the soluble fractions of spinal cords from G85R SOD-YFP or WT SOD-YFP animals of various ages were applied to anti-YFP antibody columns. After extensive washing in buffer, columns were eluted with 10 M urea in 20 mM HCl, and the products were analyzed by MudPIT, involving proteolysis with trypsin, cation exchange chromatography coupled with C18 reverse phase chromatography, and mass spectrometric analysis in a Thermo LTQ Orbitrap XL (see Experimental Procedures). As shown in the top row of Table 1, the most abundant eluted species observed was the fusion protein itself. Because equal amounts of tissue were extracted in each case, it appears that a higher amount of the fusion protein may be present in symptomatic G85R SOD-YFP cord (at 9 month age).

In addition to the fusion protein, we observed a small collective of coeluted species (Table 1). One of these proteins, the copper chaperone CCS, which normally forms a heterodimer with SOD monomer during biogenesis to deliver copper (13), was equivalently coeluted with both the mutant and wild-type fusion. In a second such partnering, endogenous mouse SOD1 was observed to be specifically captured by WT SOD-YFP, apparently forming a heterodimer with it, but the endogenous SOD1 was only marginally captured by G85R SOD-YFP, consistent with the misfolded monomeric status of the latter protein, indisposed to heterodimerize.

Soluble G85R SOD-YFP specifically captured a number of additional components. Most prominent was the molecular chaperone Hsc70, with a large number of spectral counts observed to associate with the mutant fusion protein in animals of 1, 6, and 9 months of age (Table 1). By contrast, <25% as many spectral counts of Hsc70 were associated with WT SOD-YFP. Indeed, when the fractions eluted from anti-YFP affinity capture of soluble G85R SOD-YFP and WT SOD-YFP cord extracts were directly analyzed by Western blot analysis with anti-Hsc70 antibodies, Hsc70 was exclusively observed in the G85R SOD-YFP eluate (Fig. 3 *Left*). In an additional affinity capture experiment, an SDS gel of the eluted material was directly Coomassie-stained, allowing estimation that the amount of Hsc70 recovered with G85R SOD-YFP corresponds to ≈10% the amount of the fusion protein (Fig. 3 *Right*).

In addition to association of G85R SOD-YFP with Hsc70,

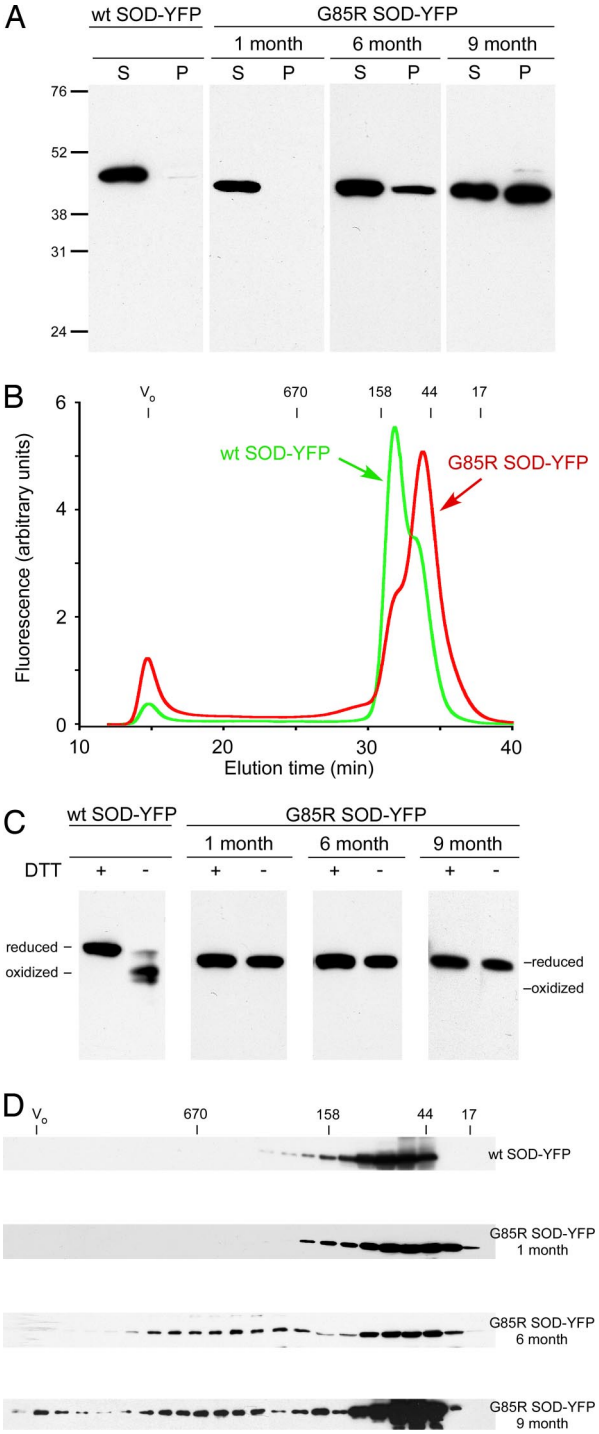

Fig. 2. Biochemical fractionation of spinal cords from WT SOD-YFP and G85R SOD-YFP animals of varying age. (*A*) Fractionation of cord extracts into soluble (S) and insoluble (P) fractions. Cords homogenized in nondenaturing buffer were centrifuged at 17,000 × *g* for 15 min and the supernatant directly solubilized in SDS sample buffer. Pellets were washed in nondenaturing buffer and then solubilized in SDS sample buffer. Identical aliquots of the fractions were loaded onto an SDS/PAGE gel. (*B*) Fractionation of soluble extracts by gel filtration on a Superose 6 column with in-line fluorescence. Note that G85R SOD-YFP migrates principally at the size of monomer whereas the WT SOD-YFP migrates at the size of a dimer. A ''shoulder'' of fluorescence migrating between 25 and 30 min was reproducibly present for the G85R SOD-YFP. (*C*) Analysis of soluble extracts prepared in iodoacetamide under reducing (+DTT) and nonreducing (−DTT) conditions. The migration positions of oxidized and reduced forms of WT SOD-YFP and G85R-YFP prepared from *Escherichia coli* under the respective conditions are indicated. As in other studies, the G85R SOD-YFP species, both reduced and oxidized, migrate in SDS/PAGE slightly more rapidly than the respective WT SOD-YFP species. Note that the insoluble fraction from a symptomatic mutant animal was also analyzed under nonreducing conditions and did not reveal higher molecular weight species that would reflect intermolecular disulfide bond formation.(*D*) Immunoblot analysis of gel filtration fractions of soluble extracts from WT SOD-YFP and G85R SOD-YFP animals. Migration position of size markers is indicated above the images. The void volume fraction (V_o) corresponds to >3 MDa.

specific elution with G85R SOD-YFP but not WT SOD-YFP was observed for 3 additional chaperone proteins, the mouse Hsp110 family members, Hspa4l, Hsph1, and Hspa4. Hsp110 proteins have recently been shown to function as nucleotide exchange factors for Hsp70 class proteins (14–17), and these 3 components seem likely to function as the normal exchangers for Hsc70. Interestingly, in mutant animals, the association of these chaperones was negligible at 1 month of age but was appreciable at 6 and 9 months. In an opposite pattern, the Hsp70 protein, Hspa1b, showed significant spectral counts at early time but lower counts at the later times. Available antibodies were not sufficiently specific to allow detection of Hsp110 and Hsp70 components by Western analysis.

Insoluble Aggregates from Mutant Cord Contain Mutant SOD-YFP and Intermediate Filament Proteins as the Major Constituents. To characterize insoluble aggregates, spinal cords from symptomatic G85R SOD-YFP animals and WT SOD-YFP animals were identically fractionated using steps of centrifugation and detergent extraction that enriched for the fluorescent aggregates from mutant cord (see *SI Methods*). This would enrich for both intracellular aggregates and fluorescent accretions from dead cells. The final fractions were subjected to MudPIT. There were 34 proteins identified with >30 spectral counts (Table S1). Most of the strongly registering proteins in the aggregate fractions are abundant cytoskeletal proteins, with the class of intermediate filament proteins (NF-M, NF-H, GFAP, and vimentin) registering strongly and mutant-specifically (see *SI Discussion* for additional considerations).

Discussion

Temporal Progression of Soluble Oligomer Formation and Aggregation of Misfolded G85R SOD-YFP. Experiments presented here with G85R SOD-YFP and wild-type SOD-YFP transgenic mice indicate that these fusion proteins, when expressed from the endogenous human SOD1 promoter, are expressed principally in motor neurons in the spinal cord, and that the G85R SOD-YFP mice specifically develop a lethal motor disease that resembles ALS, associated with late appearance of green fluorescent aggregates in motor neuron cell bodies and processes. In biochemical studies, the SOD G85R-YFP protein was observed to behave as a misfolded monomer, and the constitutive chaperone Hsc70 was observed to associate with it at all ages. Interestingly, a concurrent study of ALS-affected transgenic mice expressing a truncated SOD1 that was FLAG-tagged at its C terminus, also behaving as a misfolded monomer, showed that Hsc70 was brought down by anti-FLAG immunoprecipitation (18). Together, these data suggest that this chaperone may comprise a primary site of interaction.

A progression of misbehavior of the mutant protein in spinal cord could be observed (Fig. 4). At 1 month it was entirely soluble, associated to some degree with Hsc70, and displayed diffuse green fluorescence in neuronal cell bodies and processes. By 6 months of age it now recruited Hsp110 proteins along with Hsc70, formed soluble oligomers observed in gel filtration, and partitioned to a significant extent into the insoluble fraction. At the time motor neuron symptoms were observed at 9 months, the Hsc70/Hsp110 chaperone complexes and soluble oligomers continued to be present, but the percentage of insoluble material was

BIOCHEMISTRY

Table 1. Anti-YFP-captured proteins

Gene (protein)	G85R SOD-YFP 1 month		G85R SOD-YFP 6 months		G85R SOD-YFP 9 months		WT SOD-YFP 2 months		WT SOD-YFP 9 months	
	Spectral counts (unique)	Sequence coverage, %	Spectral counts (unique)	Sequence coverage, %	Spectral counts (unique)	Sequence coverage, %	Spectral counts (unique)	Sequence coverage, %	Spectral counts (unique)	Sequence coverage, %
SOD-YFP	3,220 (3,220)	73	4,246 (4,245)	81	7,710 (7,708)	95	3,043 (3,035)	77	4,930 (4,920)	81
Hspa8 (Hsc70)	604 (396)	49	515 (274)	70	1,328 (1,138)	80	154 (92)	42	79 (41)	42
Hspa2 (Hsp70–2)	—	—	117 (8)	26	122 (8)	27	73 (2)	18	33 (2)	15
Hspa4l (Hsp110)	3 (2)	7	67 (62)	45	101 (95)	59	—	—	—	—
Hspa1b (Hsp70–1B)	216 (1)	11	153 (15)	26	89 (16)	33	19 (4)	12	17 (4)	12
SOD1 - mouse	5 (5)	29	55 (54)	55	88 (86)	57	1,028 (1020)	64	593 (583)	82
Hsph1 (Hsp105/110)	3 (2)	3	31 (27)	30	73 (68)	46	3 (3)	3	—	—
Hspa4 (Hsp110)	7 (5)	8	53 (48)	40	46 (39)	38	—	—	—	—
Hspa5 (Grp 78)	70 (1)	6	15 (4)	12	30 (6)	12	11 (2)	9	—	—
Dnaja1 (Dnaj A1)	—	—	2 (2)	6	23 (23)	48	—	—	—	—
CCS (Copper chaperone)	10 (10)	15	12 (12)	29	21 (21)	49	12 (12)	14	13 (13)	25

Proteins identified by Mud-PIT analysis of affinity captured SOD-YFP with Spectral Counts above 20 for the G85R SOD-YFP 9 month-old sample are shown. These spectral counts represent the number of times the analysis identified a peptide corresponding to the assigned protein and can be viewed as a relative measure of protein abundance. Notably, when a peptide was common to two related proteins that were identified to be present by other unique peptides, the peptide was scored with both proteins. The spectral counts that are unique to the identified protein are shown in parenthesis. Percent sequence coverage, the percentage of the primary structure of the identified protein covered by peptides, is also reported. Dashes indicate the absence of any peptide for the indicated protein.

substantially increased, associated with the morphologic appearance of visible, green fluorescent aggregates in both neuronal cell bodies and processes.

Nature of Progression to Oligomer Formation. The cause of the progression of oligomerization and aggregation of the mutant protein remains to be determined, with the transition to soluble oligomer formation and partial insolubility between 1 month and 6 months likely to be particularly informative. Is this an effect of increasing expression of the mutant protein itself as a response of the SOD promoter? In additional in situ analyses similar to Fig. S6, the amount of mRNA appears to increase with age, but further quantitative studies will be needed to establish whether

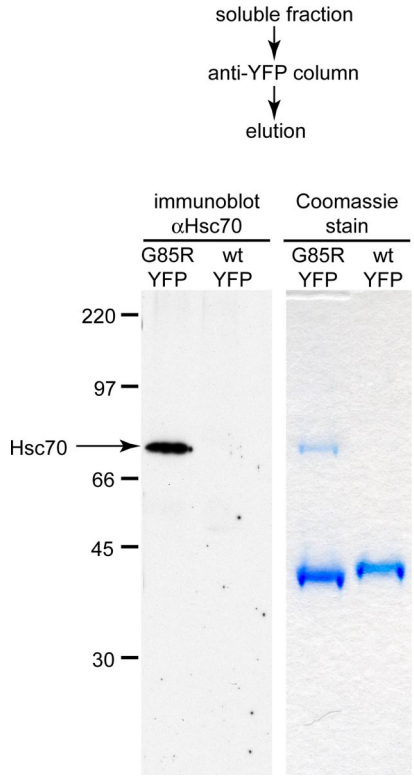

Fig. 3. Immunoblot analysis with anti-Hsc70 (*Left*) and Coomassie staining (*Right*) of fractions eluted from anti-YFP chromatography of soluble extract from spinal cord of G85R SOD-YFP and WT SOD-YFP animals. Rabbit polyclonal antibody to an Hsc70-specific peptide (SPA-816) was obtained from Assay Designs.

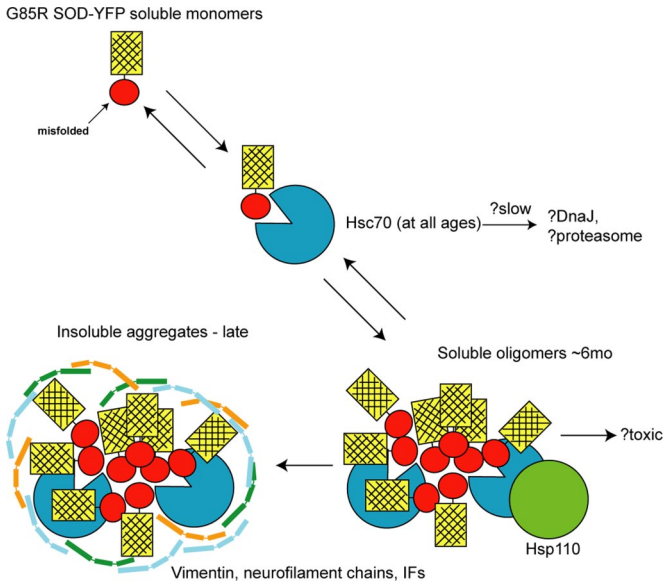

Fig. 4. Model for temporal progression of behavior of G85R SOD-YFP. At all ages the misfolded monomer, shown as a red ball, associates with the cytosolic constitutive chaperone Hsc70. In a 1-month-old animal, the mutant protein is entirely soluble as indicated by fluorescence and biochemical analyses. A fraction is likely to be trafficked to the proteasome and degraded. At 6 months, there is oligomerization and insolubility, despite detectable association at this point of Hsp110 exchange factors, presumably with Hsc70. The soluble oligomers that are formed could potentially exert toxic effects. At late time when animals are symptomatic, there are visible and readily detectable insoluble aggregates, composed, as observed here by mass spectrometry (see Table S1), principally of intermediate filaments and mutant SOD.

the level of mRNA progressively increases in the mutant setting, potentially suggestive of a positive feedback effect of misfolding/stress upon the SOD promoter itself. An alternative explanation of the progression to aggregation is a potential effect of aging on the chaperone/proteolytic system that is the likely cellular mechanism for handling the mutant protein. An age-related decline in 1 or more such components could herald the decompensation. Whatever the answer, it is striking that a stress response is not mounted at any point against the mutant protein, at least as judged by the lack of binding of stress-responsive proteins to it, despite it being present at the level of a few percent of soluble protein in motor neurons. (Typically $\approx$10 μg of fusion protein was recovered per spinal cord of a total of $\approx$800 μg of soluble protein). Although we observed a small level of associated Hsp70 and Grp78 in 1-month-old mutant animals, the amounts recovered were reduced at later times (Table 1). We note further that a UPR response was not present in symptomatic mutant animals (Fig. S7), contrasting with the reports in refs. 19 and 20.

Ubiquitination and Degradation of Misfolded G85R SOD-YFP. The fate of Hsc70-bound G85R SOD-YFP protein in 1-month-old "compensated" animals is of interest to consider. A dynamic Hsc70-DnaJ cycle could function to maintain the misfolded protein in a soluble state. Presumably, however, the misfolded protein must ultimately be turned over. How efficiently is it "handed off" to the proteolytic apparatus as opposed to cycling on and off of Hsc70? Interestingly, the level of ubiquitination of both the G85R and the wild-type SOD-YFP fusion protein was relatively low in 1- to 2-month-old animals but rose substantially in both cases by 6–9 months of age, with ubiquitin modification occurring at the later times principally on lysine 10 of the SOD moiety (Table S2). With respect to turnover, we are currently measuring rates for both the mutant and wild-type fusion proteins in vivo. Notably, however, G85R SOD has been observed to turn over at a more rapid rate than wild-type SOD in cell culture studies (21). This seems inconsistent with the observations of significant diffuse fluorescence in neuronal cell bodies in mutant transgenic animals but not wild-type at 1 and 6 months of age. Perhaps, however, the observed fluorescence in neuron cell bodies of our mutant animals reflects slow diffusion of the mutant protein, as opposed to slow turnover. The nature of neurotoxicity of the mutant fusion protein, possibly conferred by soluble oligomers (refs. 22 and 23, but see also ref. 8), also remains unclear. Concerning cellular targets of toxicity, as mentioned, we failed to observe a UPR response in symptomatic animals (Fig. S7), and we also did not detect abnormalities of mitochondria, which appeared morphologically normal upon EM inspection and did not exhibit significant fluorescence when isolated (data not shown). Thus, the nature of toxicity remains to be resolved.

Experimental Procedures

In general, at least 4 animals were examined for each of the analyses presented, with the exception of studies of 1-month-old mutant animals, where only 2 or 3 were used. Representative images and experiments are presented.

Tissue Microscopy. Fluorescent microscopy was performed on spinal cords embedded in OCT (Sakura Finetek) and frozen in 2-methybutane cooled with liquid nitrogen and stored at -80 °C. Frozen tissue was sectioned (20 μm), using a Leica CM3000 Cryostat at -20 °C and preserved with Vectashield (VectorLabs). The tissue was observed using the green filter on an Axioskop2 Plus microscope (Zeiss).

Biochemical Analysis. Spinal cords from transgenic mice of various ages were homogenized on ice in 0.5 mL of PBS containing 1 mM each EDTA, EGTA, and TCEP, and 1 tablet/ml of Complete protease inhibitor mixture (Roche). After centrifugation at 17,000 $\times$ *g* for 15 min, the supernatant was fractionated on a gel filtration column (Superose 6; GE Healthcare), eluted with PBS. Fractions were analyzed by SDS/PAGE and Western blot analysis, using an affinity-purified rabbit polyclonal antibody to YFP.

Affinity Capture and Mass Spectrometry. Supernatant fractions were subjected to affinity-capture, using the anti-YFP antibody cross-linked with DSS to Ultralink protein A (Thermo-Fisher). After extensive washing in PBS, affinity-captured proteins were eluted using 20 mM HCl, 10 M urea, then neutralized by addition of Tris (pH 8), to 200 mM. The eluted samples were reduced and alkylated with 2 mM TCEP and 10 mM iodoacetamide. MudPIT analysis was then carried out as described in ref. 24, using an LTQ Orbitrap XL mass spectrometer (Thermo-Fisher). Data were analyzed using SEQUEST, and were then inspected with DTASelect (25).

ACKNOWLEDGMENTS. We thank David Borchelt for a human SOD1 genomic clone, Mikael Oliveberg for plasmids directing expression of human SOD1 in *E. coli*, David Sarracino for help with initial proteomic studies, Gordon Terwilliger for technical help, and Wayne Fenton for helpful discussion. This work was supported by Howard Hughes Medical Institute and NIH.

1. Bruijn LI, Miller TM, Cleveland DW (2004) Unraveling the mechanisms involved in motor neuron degeneration in ALS. *Annu Rev Neurosci* 27:723–749.
2. Pasinelli P, Brown RH (2006) Molecular biology of amyotrophic lateral sclerosis: Insights from genetics. *Nat Rev Neurosci* 7:710–723.
3. Lindberg MJ, Byström R, Boknäs N, Andersen PN, Oliveberg M (2005) Systematically perturbed folding patterns of amyotrophic lateral sclerosis (ALS)-associated SOD1 mutants. *Proc Natl Acad Sci USA* 102:9754–9759.
4. Valentine JS, Doucette PA, Potter SZ (2005) Copper-zinc superoxide dismutase and amyotrophic lateral sclerosis. *Annu Rev Biochem* 74:563–593.
5. Hart PJ (2006) Pathogenic superoxide dismutase structure, folding, aggregation and turnover. *Curr Op Chem Biol* 10:131–138.
6. Svensson AK, Bilsel O, Kondrashkina E, Zitzewitz JA, Matthews CR (2006) Mapping the folding free energy surface for metal-free human Cu,Zn superoxide dismutase. *J Mol Biol* 364:1084–1102.
7. Reaume AG, *et al.* (1996) Motor neurons in Cu/Zn superoxide dismutase-deficient mice develop normally but exhibit enhanced cell death after axonal injury. *Nat Genet* 13:43–47.
8. Matsumoto G, Stojanovic A, Holmberg CI, Kim S, Morimoto RI (2005) Structural properties and neuronal toxicity of amyotrophic lateral sclerosis-associated Cu/Zn superoxide dismutase 1 aggregates. *J Cell Biol* 171:75–85.
9. Rosen DR, *et al.* (1993) Mutations in Cu/Zn superoxide dismutase gene are associated with familial amyotrophic lateral sclerosis. *Nature* 362:59–62.
10. Bruijn LI, *et al.* (1997) ALS-linked SOD1 mutant G85R mediates damage to astrocytes and promotes rapidly progressive disease with SOD1-containing inclusions. *Neuron* 18:327–338.
11. Zetterström P, *et al.* (2007) Soluble misfolded subfractions of mutant superoxide dismutase-1s are enriched in spinal cords throughout life in murine ALS models. *Proc Natl Acad Sci USA* 104:14157–14162.
12. Jonsson PA, *et al.* (2006) Disulphide-reduced superoxide dismutase-1 in CNS of transgenic amyotrophic lateral sclerosis models. *Brain* 129:451–464.
13. Lamb AL, Torres AS, O'Halloran TV, Rosenzweig AC (2001) Heterodimeric structure of superoxide dismutase in complex with its metallochaperone. *Nat. Struct Biol* 8:751–755.
14. Raviol H, Sadlish H, Rodriguez F, Mayer MP, Bukau B (2006) Chaperone network in the yeast cytosol: Hsp110 is revealed as an Hsp70 nucleotide exchange factor. *EMBO J* 25:2510–2518.
15. Dragovic Z, Broadley SA, Shomura Y, Bracher A, Hartl FU (2006) Molecular chaperones of the Hsp110 family act as nucleotide exchange factors of Hsp70s. *EMBO J* 25:2519–2528.
16. Schuermann JP, *et al.* (2008) Structure of the Hsp110:Hsc70 nucleotide exchange machine. *Mol Cell* 31:232–243.
17. Polier S, Dragovic Z, Hartl FU, Bracher A (2008) Structural basis for the cooperation of Hsp70 and Hsp110 chaperones in protein folding. *Cell* 133:1068–1079.
18. Watanabe Y, *et al.* (2008) Adherent monomer-misfolded SOD1. *PLoS ONE* 3:e3497.
19. Kikuchi H, *et al.* (2006) Spinal cord endoplasmic reticulum stress associated with a microsomal accumulation of mutant superoxide dismutase-1 in an ALS model. *Proc Natl Acad Sci USA* 103:6025–6030.
20. Nishitoh H, *et al.* (2008) ALS-linked mutant SOD1 induces ER stress- and ASK1-dependent motor neuron death by targeting Derlin-1. *Genes Dev* 22:1451–1464.
21. Borchelt DR, *et al.* (1995) Superoxide dismutase 1 subunits with mutations linked to familial amyotrophic lateral sclerosis do not affect wild-type subunit function. *J Biol Chem* 270:3234–3238.
22. Bucciantini M, *et al.* (2002) Inherent toxicity of aggregates implies a common mechanism for protein misfolding diseases. *Nature* 416:507–511.
23. Shankar GM, *et al.* (2008) Amyloid-β protein dimers isolated directly from Alzheimer's brains impair synaptic plasticity and memory. *Nature Med* 14:837–842.
24. Washburn MP, Wolters D, Yates JR, III (2001) Large-scale analysis of the yeast proteome by multidimensional protein identification technology. *Nat Biotech* 19:242–247.
25. Tabb DL, McDonald WH, Yates JR, III (2002) DTASelect and Contrast: Tools for assembling and comparing protein identifications from shotgun proteomics. *J Proteome Res* 1:21–26.